NASA Technical Memorandum 104053
DOT/FAA/RD-91/10

A Simple, Analytical, Axisymmetric Microburst Model for Downdraft Estimation

Dan D. Vicroy

February 1991

National Aeronautics and Space Administration

Langley Research Center
Hampton, Virginia 23665-5225

U.S. Department of Transportation

Federal Aviation Administration

Summary

Many in the commercial aviation industry consider wind shear to be a major safety concern. NASA has been developing airborne, forward-looking, system concepts to detect hazardous wind shear. Doppler radar and LIDAR are two candidate concepts being tested to provide this capability. An inherent limitation of this type of system is its inability to measure velocities perpendicular to the line-of-sight. Although these systems can detect the presence of a wind shear by measuring the divergence of the horizontal wind profile, their inability to measure microburst downdrafts can result in a significant underestimate of the magnitude of the hazard. However, the vertical wind component can be inferred from the horizontal wind profile through theoretical or empirical analytical models of microbursts. A simple analytical microburst model has been developed for use in estimating vertical winds from horizontal wind measurements. It is an axisymmetric, steady state model that uses shaping functions to satisfy the mass continuity equation and simulate boundary layer effects. The model is defined through four model variables: the radius and altitude of the maximum horizontal wind, a shaping function variable, and a scale factor. The model closely agrees with a high-fidelity analytical model and measured data, particularly in the radial direction and at lower altitudes. At higher altitudes, the model tends to overestimate the wind magnitude, relative to the measured data.

Introduction

Many in the commercial aviation industry consider wind shear to be a major safety concern. Wind shear is a rapid change in wind velocity (speed or direction) over a relatively short distance. It can be found in a variety of weather conditions such as gust fronts, sea-breeze fronts, and mountain waves. Hazardous wind shear is most often associated with the convective outflows of thunderstorms. One such convective activity is the microburst, which is a particularly lethal form of wind shear when encountered at low altitude. The microburst is a strong localized downdraft of 2 to 10 minute duration, which causes a significant outflow as it impacts the ground.

The hazard of wind shear arises principally from its deceptive nature. In a typical microburst encounter, the airplane initially experiences a performance increasing headwind as it penetrates the outflow region of the microburst. This will cause either an increase in the airplane's airspeed or a deviation above the intended flight path, or both. Sensing this, the pilot may take corrective action to return to the intended flight path. This is normally achieved by reducing thrust and pitch resulting in a reduction in the energy of the airplane. As the airplane enters the core of the microburst, there is a rapid decrease in headwind, shifting to a tailwind. This is accompanied by a strong downdraft. The combination of these wind changes tends to reduce airspeed and push the airplane toward the ground. If the energy of the airplane is sufficiently low it may not be able to recover from the encounter.

The Federal Aviation Administration, as lead agency for civil aviation safety, has established an integrated wind shear program plan aimed at reducing the hazard of low-level wind shear. The program plan incorporates the expertise of industry, universities, and various government agencies such as the National Aeronautics and Space Administration (NASA), the National Oceanic and Atmospheric Administration, and the Department of Defense into a multi-year research and development effort. The objective of NASA's contribution to the wind shear program is to provide the technology base to reduce the risk of low-altitude wind shear through airborne detection, warning, and avoidance. Key elements of the NASA research effort include characterization of the wind shear phenomena in the aviation context, airborne remote-sensor technology that provides forward-looking avoidance capability, and flight-management system concepts that provide timely and accurate transfer of weather hazard information to flight crews. The direction of the NASA research thrust is toward developing system concepts that embrace forward-looking sensor technology. Thus providing the flight crew with awareness of the presence of wind shear with enough time to avoid the affected area or escape from the encounter.

A fundamental requirement for a forward-looking, airborne wind shear detection system is the ability to estimate reliably the magnitude of the wind shear hazard that would be experienced by an airplane if it were to continue along the line-of-sight. The hazard is a function of both the horizontal and vertical wind components. Doppler radar and LIDAR are two candidate concepts being tested to provide this capability. Both systems measure the Doppler shift from aerosols, rain drops and other debris in the air to determine the line-of-sight relative velocity of the air. An inherent limitation of this type of system is its inability to measure velocities perpendicular to the line-of-sight. Although these systems can detect the presence of a microburst by measuring the divergence of the horizontal wind profile, their inability to measure the downdraft can result in a significant underestimate of the magnitude of the hazard. However, the vertical wind component can be inferred from the horizontal wind profile through theoretical or empirical analytical models of microbursts. The simple analytical model described in this report was developed for this purpose.

Symbols

r radial coordinate (distance from downburst center), meters

u wind velocity in the x-direction, m/sec

u_r wind velocity in the r-direction, m/sec

v wind velocity in the y-direction, m/sec

w wind velocity in the z-direction, m/sec

x longitudinal coordinate, meters

y lateral coordinate, meters

z vertical coordinate (positive up), meters

Model Development

The analytical microburst model described in this report is a modification of the Oseguera/Bowles downburst model described in reference 1. The Oseguera/Bowles model was developed as a simple analytical microburst model for use in studying wind shear escape procedures. It is an axisymmetric, steady state model that uses shaping functions to satisfy the mass continuity equation and simulate boundary layer effects. The following describes the derivation of this model and the subsequent modifications.

The axisymmetric, steady state mass continuity equation expressed in cylindrical coordinates is:

$$\frac{\partial u_r}{\partial r} + \frac{\partial w}{\partial z} + \frac{u_r}{r} = 0 \tag{1}$$

This equation can be satisfied by solutions of the form:

$$u_r = f(r)p(z) \tag{2}$$

$$w = g(r^2)q(z) \tag{3}$$

provided

$$\frac{\partial [rf(r)]}{\partial r^2} = \frac{\lambda}{2} g(r^2) \tag{4}$$

$$\frac{\partial q(z)}{\partial z} = -\lambda p(z) \tag{5}$$

where

$f(r)$ radial shaping function of the horizontal wind velocity, m/sec

$g(r^2)$ radial shaping function of the vertical wind velocity

$p(z)$ vertical shaping function of the horizontal wind velocity

$q(z)$ vertical shaping function of the vertical wind velocity, m/sec

λ scaling factor, 1/sec

The shaping functions selected for the Oseguera/Bowles model were:

$$f(r) = \frac{\lambda R^2}{2r}\left[1 - e^{-(r^2/R^2)}\right] \tag{6}$$

$$g(r^2) = e^{-(r^2/R^2)} \tag{7}$$

$$p(z) = e^{-(z/z^*)} - e^{-(z/\epsilon)} \tag{8}$$

$$q(z) = -\lambda\left\{\epsilon\left[e^{-(z/\epsilon)} - 1\right] - z^*\left[e^{-(z/z^*)} - 1\right]\right\} \tag{9}$$

where

R radius of downburst shaft, meters

z^* characteristic height (out of boundary layer), meters

ϵ characteristic height (in boundary layer), meters

Figures 1 and 2 show the characteristic shape of these functions.

The resultant horizontal and vertical wind equations for the Oseguera/Bowels model were obtained by combining these shaping functions.

$$u_r = \frac{\lambda R^2}{2r}\left[1 - e^{-(r^2/R^2)}\right]\left[e^{-(z/z^*)} - e^{-(z/\epsilon)}\right] \tag{10}$$

$$w = -\lambda e^{-(r^2/R^2)}\left\{\epsilon\left[e^{-(z/\epsilon)} - 1\right] - z^*\left[e^{-(z/z^*)} - 1\right]\right\} \tag{11}$$

This model was initially considered for use in estimating the downdraft from measured horizontal winds. The downdraft is estimated by searching for the model variable values that yield the best fit of the model to the measured horizontal winds and then using these values to compute the downdraft. The Oseguera/Bowles model was found to be ill suited for this purpose. The radial shaping function of the horizontal wind $f(r)$ was sufficiently different from the characteristic horizontal wind profile of a microburst that it was difficult to achieve a good fit to the measured winds. This then resulted in an inaccurate downdraft estimate. The modification of the Oseguera/Bowles model involved defining a new $f(r)$ that more accurately matched the characteristic horizontal wind profile of a microburst. The new shaping function was defined as:

$$f(r) = \frac{\lambda r}{2} e^{\left[\frac{1-(r^2/\beta^2)^\alpha}{\alpha}\right]} \tag{12}$$

where

α shaping function variable

β shaping function variable, meters

The radial shaping function of the vertical wind $g(r^2)$ is derived from equation 4 which can be written as:

$$g(r^2) = \frac{2}{\lambda}\frac{\partial [rf(r)]}{\partial r^2} \tag{13}$$

or

$$g(r^2) = \left[1 - \left(\frac{r^2}{\beta^2}\right)^{\alpha}\right] e^{\left[\frac{1-(r^2/\beta^2)^{\alpha}}{\alpha}\right]} \tag{14}$$

Figure 3 shows the characteristic shape of the new $f(r)$ and $g(r^2)$ functions. The vertical shaping functions $p(z)$ and $q(z)$ were not changed. The new horizontal and vertical wind equations are:

$$u_r = \frac{\lambda r}{2}\left[e^{-(z/z^*)} - e^{-(z/\epsilon)}\right] e^{\left[\frac{1-(r^2/\beta^2)^{\alpha}}{\alpha}\right]} \tag{15}$$

$$w = -\lambda\left\{\epsilon\left[e^{-(z/\epsilon)} - 1\right] - z^*\left[e^{-(z/z^*)} - 1\right]\right\} \times \left[1 - \left(\frac{r^2}{\beta^2}\right)^{\alpha}\right] e^{\left[\frac{1-(r^2/\beta^2)^{\alpha}}{\alpha}\right]} \tag{16}$$

Model Characteristics

The radius of the peak horizontal wind (r_p) at a given altitude (z) can be derived by setting the partial derivative of u with respect to r equal to zero and solving for r_p. This results in an equation of the form:

$$\left(\frac{r_p^2}{\beta^2}\right)^{\alpha} = \frac{1}{2} \tag{17}$$

or

$$r_p = \sqrt[2\alpha]{\frac{1}{2}\beta^{2\alpha}} \tag{18}$$

Therefore

$$\beta = \sqrt[2\alpha]{2r_p^{2\alpha}} \tag{19}$$

The altitude of the maximum horizontal wind z_m is dependent on the shaping functions $p(z)$ and $q(z)$. These functions were not changed from those of reference 1, where it was shown that:

$$z_m = \frac{z^*\epsilon}{z^* - \epsilon}\ln\left(\frac{z^*}{\epsilon}\right) \tag{20}$$

and

$$\frac{z_m}{z^*} = 0.22 \tag{21}$$

which yields

$$\frac{z^*}{\epsilon} = 12.5 \tag{22}$$

The velocities u_r and w can be expressed in terms of r_p, z_m, the shaping variable α, and the scale factor λ by combining equations 19, 21 and 22 with equations 15 and 16.

$$u_r = \frac{\lambda r}{2}\left[e^{c_1(z/z_m)} - e^{c_2(z/z_m)}\right] e^{\left[\frac{2-(r^2/r_p^2)^{\alpha}}{2\alpha}\right]} \tag{23}$$

$$w = -\lambda\left\{\frac{z_m}{c_1}\left[e^{c_1(z/z_m)} - 1\right] - \frac{z_m}{c_2}\left[e^{c_2(z/z_m)} - 1\right]\right\} \times \left[1 - \frac{1}{2}\left(\frac{r^2}{r_p^2}\right)^{\alpha}\right] e^{\left[\frac{2-(r^2/r_p^2)^{\alpha}}{2\alpha}\right]} \tag{24}$$

where

$$c_1 = -0.22 \tag{25}$$

$$c_2 = -2.75 \tag{26}$$

The equations for the wind along a radial can be normalized by dividing u_r by the peak horizontal wind u_p, and w by the downdraft at the center of the microburst w_0.

$$\frac{u_r}{u_p} = \frac{r}{r_p} e^{\left[\frac{1-(r^2/r_p^2)^{\alpha}}{2\alpha}\right]} \tag{27}$$

$$\frac{w}{w_0} = \left[1 - \frac{1}{2}\left(\frac{r^2}{r_p^2}\right)^{\alpha}\right] e^{\left[\frac{-(r^2/r_p^2)^{\alpha}}{2\alpha}\right]} \tag{28}$$

where

$$u_p = \frac{\lambda r_p}{2}\left[e^{c_1(z/z_m)} - e^{c_2(z/z_m)}\right] e^{(1/2\alpha)} \tag{29}$$

$$w_0 = -\lambda e^{(1/\alpha)} \times \left\{\frac{z_m}{c_1}\left[e^{c_1(z/z_m)} - 1\right] - \frac{z_m}{c_2}\left[e^{c_2(z/z_m)} - 1\right]\right\} \tag{30}$$

From equations 27 and 28 it can be seen that the shape of the normalized form of the wind equations is only dependent on the value of the shaping variable α. Figures 4 and 5 show how α effects the shape of the normalized horizontal and vertical wind functions,

respectively. Increasing α tends to steepen the rate of decay of the horizontal winds and increase the updraft of the vertical winds (updraft $= w/w_0 < 0$).

Figures 6 and 7 show how the normalized horizontal and vertical winds compare with other models and measured data. The TASS (Terminal Area Simulation System) mean profile data is the average of eight axisymmetric microburst simulations taken at or near the time of maximum outflow velocity. TASS is a numerical, time-dependent, multi-dimensional, nonhydrostatic cloud model which has been used extensively in the study of microbursts (refs. 2 and 3). The TASS vertical wind data presented in figure 7 was taken at an altitude of 500 meters. The JAWS (Joint Airport Weather Studies) mean profile shown in figure 6 is radar measured data taken from reference 4.

The Oseguera/Bowles model, shown in figures 6 and 7, considerably overestimates the horizontal winds while underestimating the vertical winds. This was the primary reason for developing the new shaping function. With $\alpha = 2$, the new model more closely models the horizontal wind decay while avoiding the excessive updrafts which result from larger values of α.

The altitude dependent shaping functions, $p(z)$ and $q(z)$, were not changed from those used in the Oseguera/Bowles model. Therefore the vertical profiles of the normalized horizontal and vertical winds were unchanged. Figures 8 and 9 show a comparison of these profiles with radar measured values. Presented in figure 8 is the peak horizontal wind at each altitude (u_p) normalized by the overall maximum horizontal wind (u_m), plotted against the altitude (z) normalized by the altitude of maximum horizontal wind (z_m). The equation for the model derived u_m is:

$$u_m = \frac{\lambda r_p}{2}\left(e^{c_1} - e^{c_2}\right)e^{(1/2\alpha)} \qquad (31)$$

Presented in figure 9 is the vertical profile of the downdraft at the core of the microburst (w_0) normalized by the core downdraft value at the altitude of maximum horizontal velocity (w_{0m}). The equation for the model derived w_{0m} is:

$$w_{0m} = -\lambda\left\{\frac{z_m}{c_1}\left[e^{c_1} - 1\right] - \frac{z_m}{c_2}\left[e^{c_2} - 1\right]\right\}e^{(1/\alpha)} \qquad (32)$$

The NIMROD (Northern Illinois Meteorological Research On Downbursts) data presented in figures 8 and 9 are Doppler radar measured winds of a microburst event presented in reference 5 (figure 30). The microburst translational speed of 15 m/s was subtracted from the horizontal wind speed.

The model agrees closely with the measured data presented in figures 8 and 9, particularly at lower altitudes. At higher altitudes, the model tends to overestimate the wind magnitude, relative to the NIMROD data.

This model was developed to estimate the downdraft from horizontal velocity measurements. However, it could also be used in a similar manner as the Oseguera/Bowles model, as a simple microburst simulation model. The equations required to use this model for microburst simulation are provided in the appendix.

Concluding Remarks

A simple analytical microburst model has been developed for use in estimating vertical winds from horizontal wind measurements. It is an axisymmetric, steady state model that uses shaping functions to satisfy the mass continuity equation and simulate boundary layer effects. The model is defined through four model variables: the radius and altitude of the maximum horizontal wind, a shaping function variable, and a scale factor. The model closely agrees with a high-fidelity analytical model (TASS) and measured data (JAWS, NIMROD), particularly in the radial direction and at lower altitudes. At higher altitudes, the model tends to overestimate the wind magnitude, relative to the NIMROD data.

References

1. Oseguera, Rosa M.; Bowles, Roland L.: *A Simple, Analytic 3-Dimensional Downburst Model Based on Boundary Layer Stagnation Flow.* NASA TM-100632, July 1988.
2. Proctor, F. H.: *The Terminal Area Simulation System, Volume I: Theoretical Formulation.* NASA CR-4046, April 1987.
3. Proctor, F. H.: *The Terminal Area Simulation System, Volume II: Verification Cases.* NASA CR-4047, April 1987.
4. Hjelmfelt, M. R.: Structure and Life Cycle of Microburst Outflows Observed in Colorado. *Journal of Applied Meterology*, Vol. 27, 1988, pp. 90.
5. Fujita, T. Theodore: Tornadoes and Downbursts in the Context of Generalized Planetary Scales. *Journal of the Atmospheric Sciences*, Vol. 38, August 1981, pp. 1511-1534.

Appendix

Microburst Model Simulation Equations

Provided below are equations for the wind velocities and their spatial derivatives at the point P in the coordinate system shown in sketch a. The microburst center is located at the origin of the axis system.

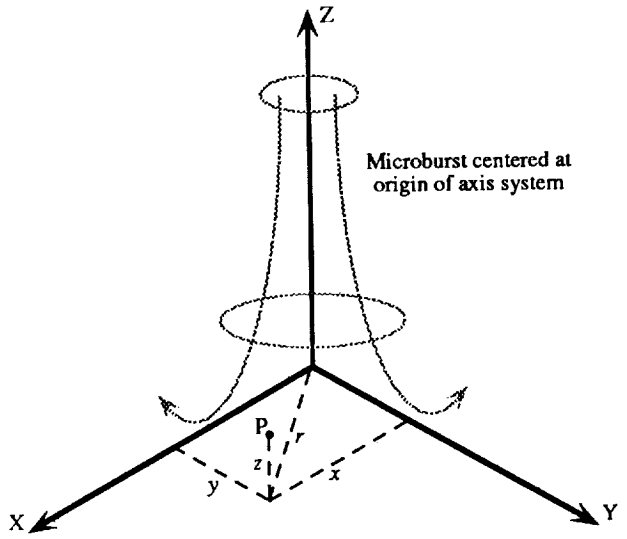

Sketch a. Coordinate system.

Model Variables

This model can be fully defined by specifying the radius, altitude and magnitude of the maximum outflow (r_p, z_m and u_m, respectively), and the value of the shaping variable α ($\alpha = 2$ is recommended). The scale factor λ can then be determined from:

$$\lambda = \frac{2u_m}{r_p\left(e^{c_1} - e^{c_2}\right)e^{(1/2\alpha)}} \qquad (A1)$$

where

$$c_1 = -0.22 \qquad (A2)$$

$$c_2 = -2.75 \qquad (A3)$$

Velocity Equations

$$u = \frac{\lambda x}{2}\left[e^{c_1(z/z_m)} - e^{c_2(z/z_m)}\right] e^{\left[\frac{2-\left(x^2+y^2\right)^{\alpha}/r_p{}^{2\alpha}}{2\alpha}\right]} \qquad (A4)$$

$$v = \frac{\lambda y}{2}\left[e^{c_1(z/z_m)} - e^{c_2(z/z_m)}\right] e^{\left[\frac{2-\left(x^2+y^2\right)^{\alpha}/r_p{}^{2\alpha}}{2\alpha}\right]} \qquad (A5)$$

$$w = -\lambda\left\{\frac{z_m}{c_1}\left[e^{c_1(z/z_m)} - 1\right] - \frac{z_m}{c_2}\left[e^{c_2(z/z_m)} - 1\right]\right\} \times \left[1 - \frac{\left(x^2+y^2\right)^{\alpha}}{2r_p{}^{2\alpha}}\right] e^{\left[\frac{2-\left(x^2+y^2\right)^{\alpha}/r_p{}^{2\alpha}}{2\alpha}\right]} \qquad (A6)$$

Spatial Derivatives

$$\frac{\partial u}{\partial x} = \frac{\lambda}{2}\left[e^{c_1(z/z_m)} - e^{c_2(z/z_m)}\right]\left[1 - \frac{x^2\left(x^2+y^2\right)^{\alpha-1}}{r_p{}^{2\alpha}}\right] \times e^{\left[\frac{2-\left(x^2+y^2\right)^{\alpha}/r_p{}^{2\alpha}}{2\alpha}\right]} \qquad (A7)$$

$$\frac{\partial u}{\partial y} = \frac{-\lambda xy\left(x^2+y^2\right)^{\alpha-1}}{2r_p{}^{2\alpha}}\left[e^{c_1(z/z_m)} - e^{c_2(z/z_m)}\right] \times e^{\left[\frac{2-\left(x^2+y^2\right)^{\alpha}/r_p{}^{2\alpha}}{2\alpha}\right]} \qquad (A8)$$

$$\frac{\partial u}{\partial z} = \frac{\lambda x}{2}\left[\left(\frac{c_1}{z_m}\right)e^{c_1(z/z_m)} - \left(\frac{c_2}{z_m}\right)e^{c_2(z/z_m)}\right] \times e^{\left[\frac{2-\left(x^2+y^2\right)^{\alpha}/r_p{}^{2\alpha}}{2\alpha}\right]} \qquad (A9)$$

$$\frac{\partial v}{\partial x} = \frac{\partial u}{\partial y} \tag{A10}$$

$$\frac{\partial v}{\partial y} = \frac{\lambda}{2}\left[e^{c_1(z/z_m)} - e^{c_2(z/z_m)}\right]\left[1 - \frac{y^2(x^2+y^2)^{\alpha-1}}{r_p{}^{2\alpha}}\right] \times e^{\left[\frac{2-(x^2+y^2)^{\alpha}/r_p{}^{2\alpha}}{2\alpha}\right]} \tag{A11}$$

$$\frac{\partial v}{\partial z} = \frac{\lambda y}{2}\left[\left(\frac{c_1}{z_m}\right)e^{c_1(z/z_m)} - \left(\frac{c_2}{z_m}\right)e^{c_2(z/z_m)}\right] \times e^{\left[\frac{2-(x^2+y^2)^{\alpha}/r_p{}^{2\alpha}}{2\alpha}\right]} \tag{A12}$$

$$\frac{\partial w}{\partial x} = \frac{\lambda x(x^2+y^2)^{\alpha-1}}{r_p{}^{2\alpha}}\left[\alpha + 1 - \frac{(x^2+y^2)^{\alpha}}{2r_p{}^{2\alpha}}\right] \times \left\{\frac{z_m}{c_1}\left[e^{c_1(z/z_m)} - 1\right] - \frac{z_m}{c_2}\left[e^{c_2(z/z_m)} - 1\right]\right\} \times e^{\left[\frac{2-(x^2+y^2)^{\alpha}/r_p{}^{2\alpha}}{2\alpha}\right]} \tag{A13}$$

$$\frac{\partial w}{\partial y} = \frac{\lambda y(x^2+y^2)^{\alpha-1}}{r_p{}^{2\alpha}}\left[\alpha + 1 - \frac{(x^2+y^2)^{\alpha}}{2r_p{}^{2\alpha}}\right] \times \left\{\frac{z_m}{c_1}\left[e^{c_1(z/z_m)} - 1\right] - \frac{z_m}{c_2}\left[e^{c_2(z/z_m)} - 1\right]\right\} \times e^{\left[\frac{2-(x^2+y^2)^{\alpha}/r_p{}^{2\alpha}}{2\alpha}\right]} \tag{A14}$$

$$\frac{\partial w}{\partial z} = -\lambda\left[e^{c_1(z/z_m)} - e^{c_2(z/z_m)}\right]\left[1 - \frac{(x^2+y^2)^{\alpha}}{2r_p{}^{2\alpha}}\right] \times e^{\left[\frac{2-(x^2+y^2)^{\alpha}/r_p{}^{2\alpha}}{2\alpha}\right]} \tag{A15}$$

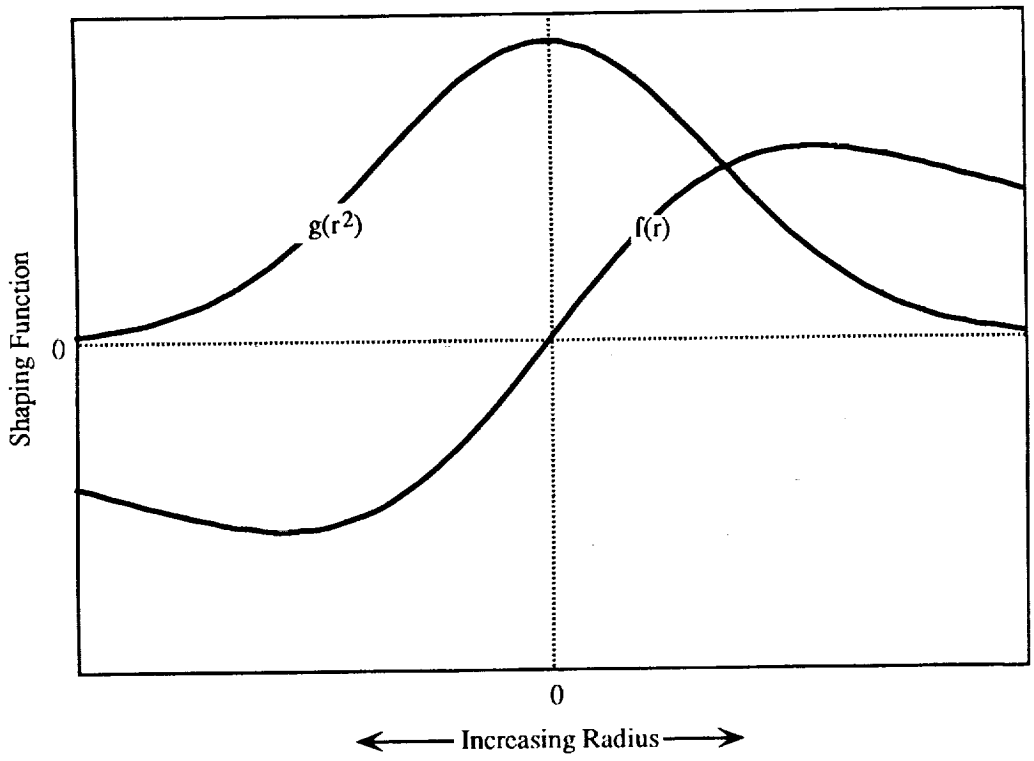

Figure 1. Characteristic variation of radial shaping functions.

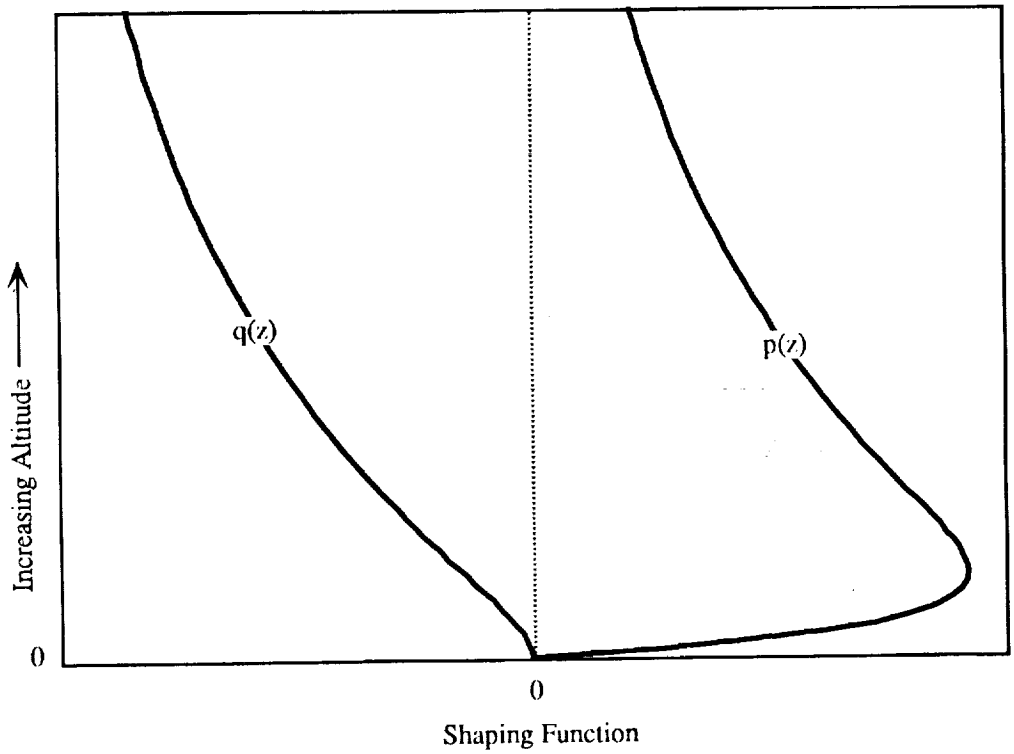

Figure 2. Characteristic variation of vertical shaping functions.

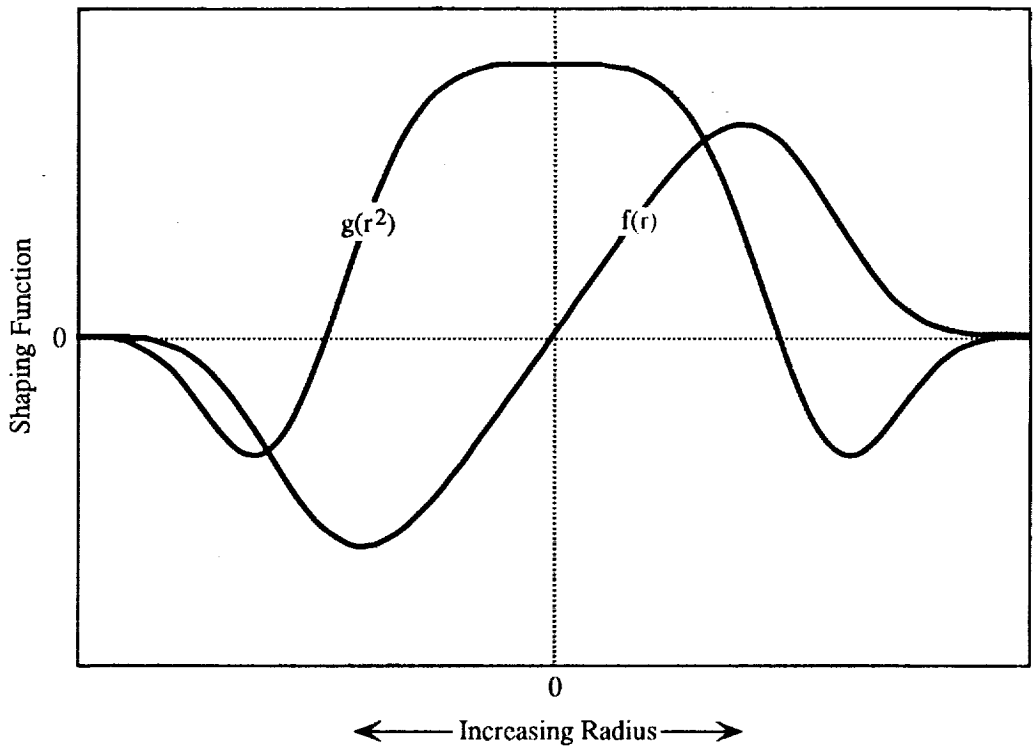

Figure 3. Characteristic variation of new radial shaping functions.

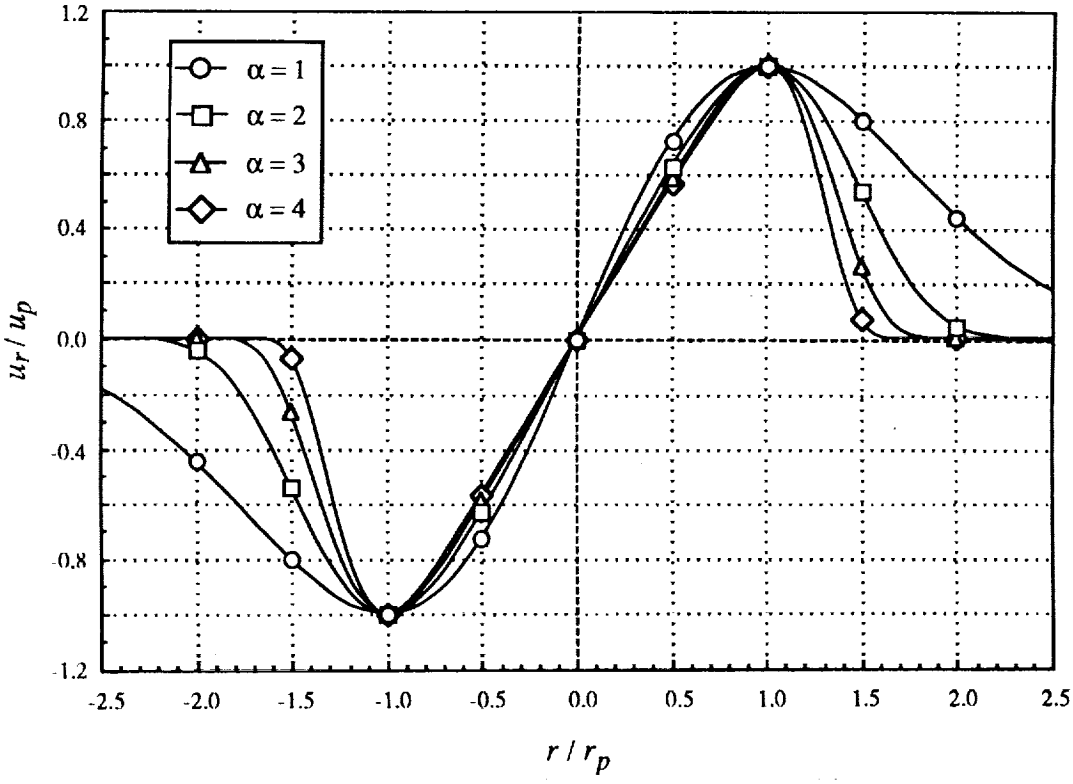

Figure 4. Normalized horizontal wind profiles for various values of α.

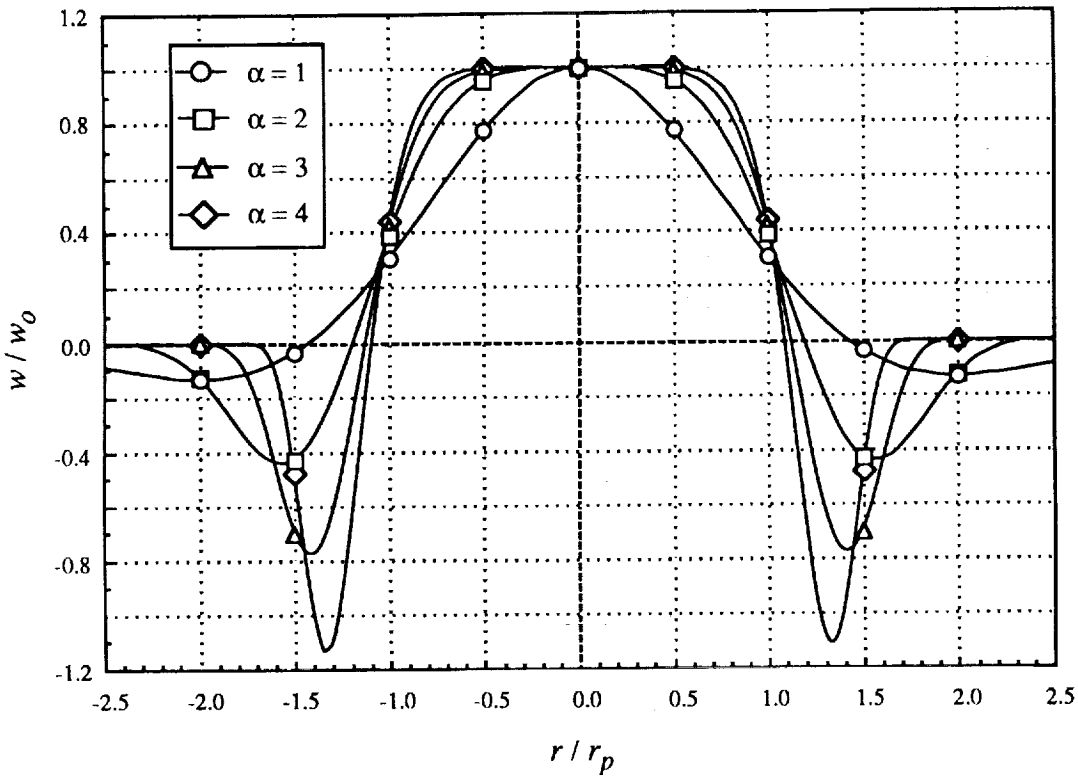

Figure 5. Normalized vertical wind profiles for various values of α.

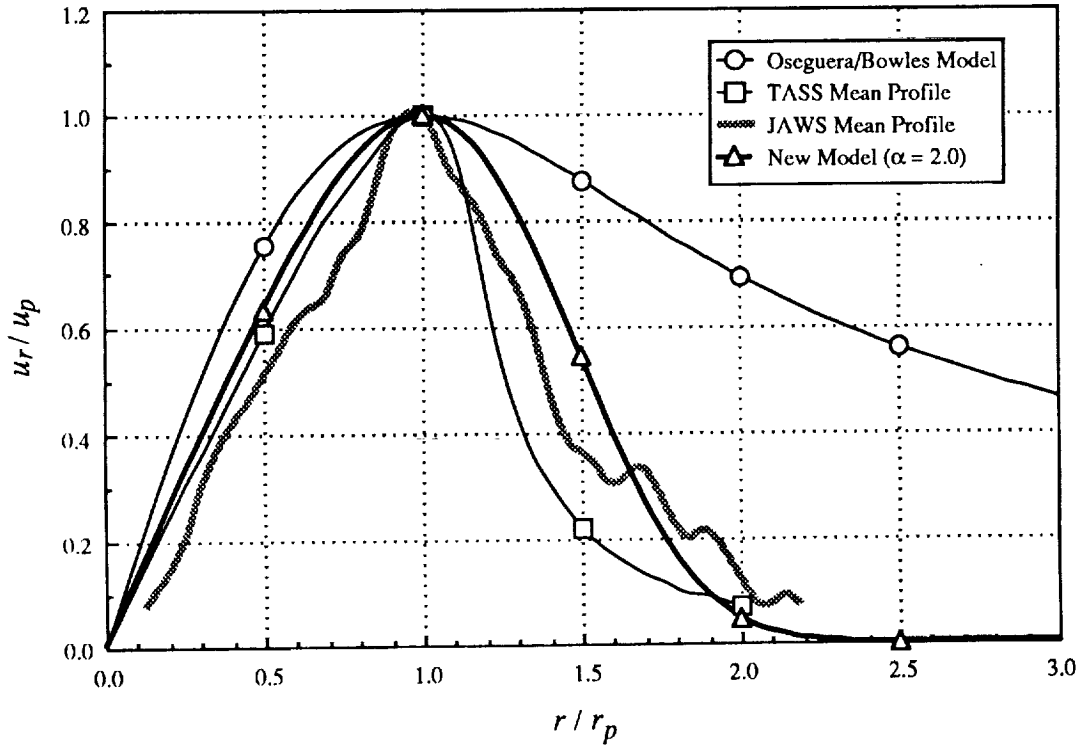

Figure 6. Comparison of normalized horizontal wind profiles along a radial.

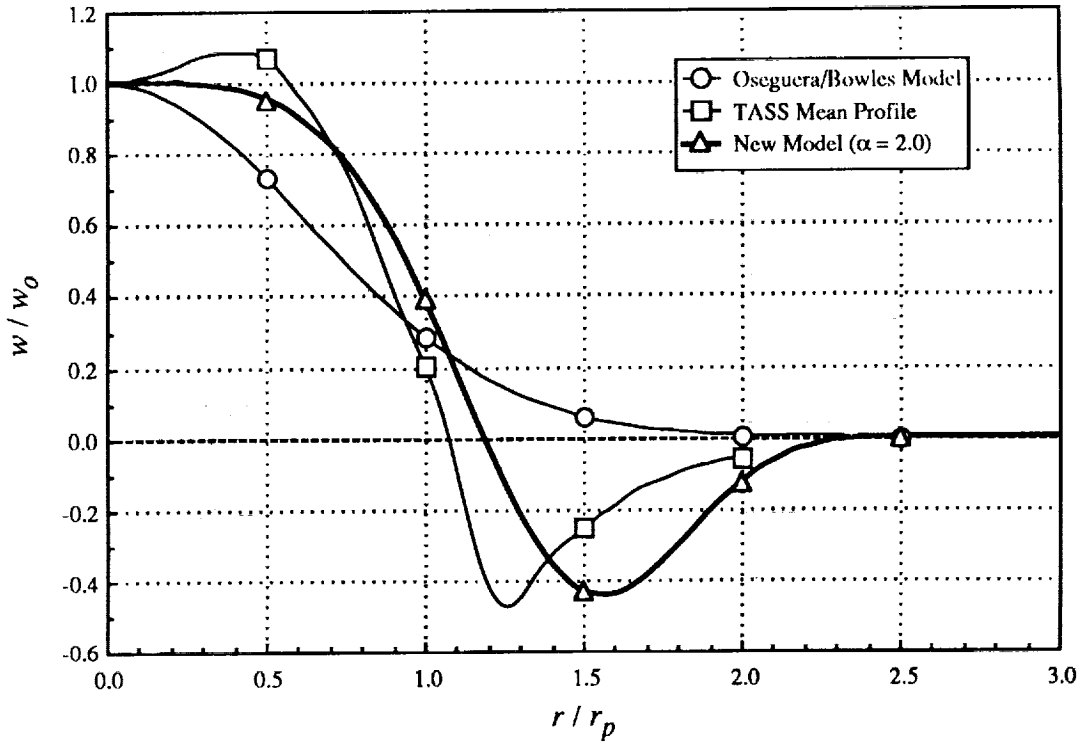

Figure 7. Comparison of normalized vertical wind profiles along a radial.

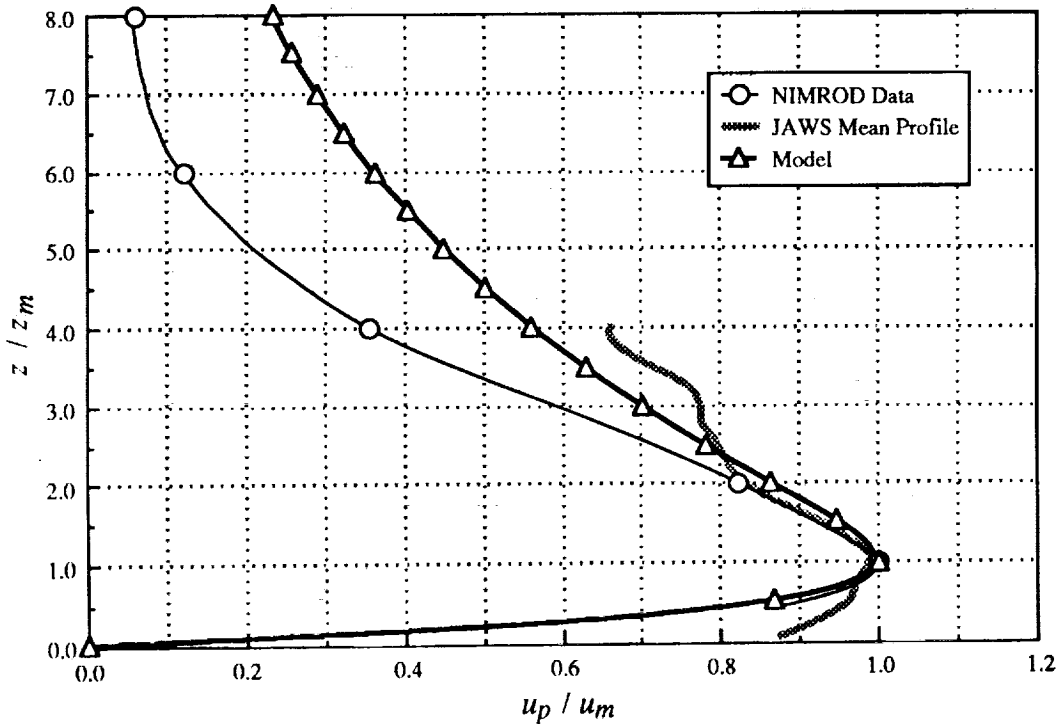

Figure 8. Comparison of the vertical profiles of the normalized horizontal winds.

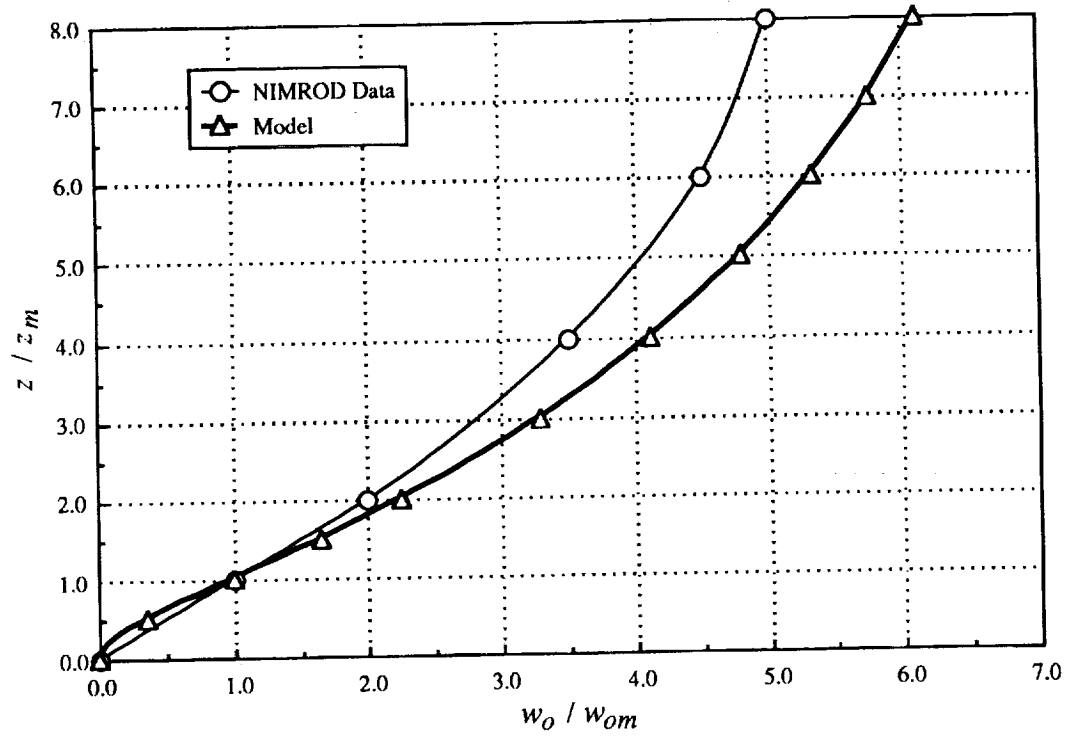

Figure 9. Comparison of the vertical profiles of the normalized vertical winds.

NASA

Report Documentation Page

1. Report No.	2. Government Accession No.	3. Recipient's Catalog No.
NASA TM-104053 DOT/FAA/RD-91/10		

4. Title and Subtitle	5. Report Date
A Simple, Analytical, Axisymmetric Microburst Model for Downdraft Estimation	February 1991
	6. Performing Organization Code

7. Author(s)	8. Performing Organization Report No.
Dan D. Vicroy	
	10. Work Unit No. 505-64-12

9. Performing Organization Name and Address	11. Contract or Grant No.
NASA Langley Research Center Hampton, VA 23665-5225	
	13. Type of Report and Period Covered Technical Memorandum

12. Sponsoring Agency Name and Address	14. Sponsoring Agency Code
National Aeronautics and Space Administration Washington, DC 20546-0001 and Department of Transportation, Washington, DC 20590	

15. Supplementary Notes

Joint NASA and FAA report.

16. Abstract

Many in the commercial aviation industry consider wind shear to be a major safety concern. NASA has been developing forward-looking system concepts to detect hazardous wind shear. Doppler radar and LIDAR are two candidate concepts being tested to provide this capability. An inherent limitation of this type of system is its inability to measure velocities perpendicular to the line-of-sight. Although these systems can detect the presence of a wind shear by measuring the divergence of the horizontal wind profile, their inability to measure the downdraft results in a significant underestimate of the magnitude of the hazard. However, the vertical wind component can be inferred from the horizontal wind profile through theoretical or empirical analytical models of microbursts. A simple analytical microburst model has been developed for use in estimating vertical winds from horizontal wind measurements. It is an axisymmetric, steady state model that uses shaping functions to satisfy the mass continuity equation and simulate boundary layer effects. The model is defined through four model variables: the radius and altitude of the maximum horizontal wind, a shaping function variable, and a scale factor. The model closely agrees with a high-fidelity analytical model and measured data, particularly in the radial direction and at lower altitudes. At higher altitudes, the model tends to overestimate the wind magnitude, relative to the measured data.

17. Key Words (Suggested by Author(s))	18. Distribution Statement
microburst downburst simulation wind shear	Unclassified---Unlimited Subject Category 05

19. Security Classif. (of this report)	20. Security Classif. (of this page)	21. No. of pages	22. Price
Unclassified	Unclassified	12	A03